

Preparation, Structure, and Properties of a New Quaternary Arsenide $\text{LaZr}_2\text{Ni}_4\text{As}_4$

EL HOUSSINE EL GHADRAOUI, JEAN-YVES PIVAN,
AND ROLAND GUÉRIN

*Université de Rennes-Beaulieu, Laboratoire de Chimie Minérale B,
Unité Associée au CNRS No. 254, Avenue du Général Leclerc,
35042 Rennes Cédex, France*

Received August 1, 1988; in revised form September 28, 1988

The quaternary arsenide $\text{LaZr}_2\text{Ni}_4\text{As}_4$ crystallizes in monoclinic symmetry, space group $P2_1/m$ with unit cell parameters $a = 9.800(3) \text{ \AA}$, $b = 3.948(1) \text{ \AA}$, $c = 9.388(4) \text{ \AA}$, and $\beta = 97.56(2)^\circ$ and two formulae per unit cell. The X-ray structure was solved and refined to a final R value of 0.035 for 936 independent reflections and 69 variable parameters. The structure consists of isolated $[\text{LaAs}_6]$ trigonal prisms, pairs of $[\text{ZrAs}_6]$ octahedra with a common edge, isolated $[\text{ZrAs}_5]$ pyramids, and $[\text{NiAs}_4]$ tetrahedra. It is the first time that such metalloid polyhedra are present simultaneously in the pnictide chemistry. Structural similarities with the structures of YCo_5P_3 , $\text{Zr}_2\text{Ni}_3\text{P}_3$, Co_2P , Fe_2As , NiAs , and NaCl are discussed in terms of localized modifications of the coordination of the metal atoms. Magnetic and electrical measurements for $\text{LaZr}_2\text{Ni}_4\text{As}_4$ showed almost temperature independent paramagnetism and metallic conduction. © 1989 Academic Press, Inc.

Introduction

Since the first ternary lanthanoid-transition metal pnictides were synthesized at the end of the 1970s (1), more than 200 compounds have been isolated, many of them with new structure types. With nickel as transition metal, materials were synthesized with the following structure types: ThCr_2Si_2 , CaBe_2Ge_2 , $\text{La}_6\text{Ni}_6\text{P}_{17}$, LaCo_5P_3 , $\text{Zr}_2\text{Fe}_{12}\text{P}_7$, $\text{Zr}_6\text{Ni}_{20}\text{P}_{13}$, $\text{Ho}_5\text{Ni}_{19}\text{P}_{12}$, $\text{Ho}_{20}\text{Ni}_{66}\text{P}_{43}$, $\text{Zr}_2\text{Ni}_3\text{P}_3$, Zr_2NiAs_2 , ZrNi_4P_2 (1-16).

Over the last 10 years, more and more crystallographic data being published, many studies have been devoted to elaborate models in order to explain the crystallochemical principles as well as the physical properties of these new materials (17,

18). Today, it is agreed that the electropositivity and the size of the metal atoms govern the stereochemistry in these compounds. In that way, the largest pnictogen sites are suitable for rare earth, zirconium, hafnium, scandium, or yttrium atoms (trigonal prisms, octahedra, etc.), when the smallest sites are occupied by transition metal atoms, such as iron, cobalt, nickel, rhodium, etc. (pyramids, tetrahedra, and triangles).

In order to verify these criteria, we tried to replace specifically the zirconium atoms by the rare-earth ones in the $\text{Zr}_2\text{Ni}_3\text{P}_3$ type, the distinctive feature of which was the occurrence of $[\text{ZrP}_6]$ trigonal prisms together with $[\text{ZrP}_6]$ octahedra (14). We were successful in replacing partially or completely

the zirconium in trigonal prismatic coordination by a rare earth to obtain the $\text{Ln}_x\text{Zr}_{2-x}\text{Ni}_3\text{X}_3$ compounds for $\text{Ln} = \text{Ce}, \text{Er}, \text{Yb}$ and $\text{X} = \text{P}, \text{As}$ (19). In contrast, attempts to synthesize such a compound in the case of lanthanum were unsuccessful; nevertheless, this study led to a new quaternary arsenide $\text{LaZr}_2\text{Ni}_4\text{As}_4$.

The present paper deals with the crystal structure and physical properties of this new arsenide and its structural relationship with other related structures is emphasized.

Experimental Details and X-Ray Structure Determination

Stoichiometric amounts of lanthanum as chips, zirconium, and nickel as powders and β -As (all minimum purity 99.9%) were weighed, then mixed and pressed into pellets in a glove box under purified argon to prevent oxidation. The mixture was then placed in alumina crucibles prior to arc-

weld sealing inside molybdenum crucibles under 0.5 atmosphere of argon. A high-temperature graphite-resistor furnace was used to reach temperatures of about 1500°C followed by slow cooling at rates of $20\text{--}50^\circ\text{C}/\text{hr}$ to room temperature. Tiny single crystals were recovered from crushed ingots and investigated on an automated four-circle Nonius CAD-4 diffractometer equipped with a graphite monochromator using $\text{MoK}\alpha$ radiation. The lattice parameters were determined from least-square refinement of 25 reflections collected with θ ranging from 6 to 22° . The symmetry was found to be monoclinic with systematic absences on $0k0$ ($k = 2n + 1$) reflections which were indicative of space group $P2_1/m$.

The crystal data and the methods used for intensity collection, structure determination, and refinement are summarized in Table I. The intensities were corrected from Lorentz and polarization effects as usual but not for absorption. Analyses by

TABLE I
CRYSTAL DATA, INTENSITY COLLECTION, AND REFINEMENT OF
 $\text{LaZr}_2\text{Ni}_4\text{As}_4$

Formula	$\text{LaZr}_2\text{Ni}_{4-x}\text{As}_4$
Molecular weight	844.136
Crystal dimensions (mm^3)	$0.18 \times 0.02 \times 0.02$
Crystal class	Monoclinic
Lattice constants (\AA)	$a = 9.800(3), b = 3.948(1), c = 9.388(4)$ $\beta = 97.56(2)^\circ$
Z	2
$d_{\text{cal.}}$ (g/cm^3)	7.78
Space group	$P2_1/m$
Radiation	$\text{MoK}\alpha = 0.7107 \text{\AA}$
Absorption coefficient (mm^{-1})	28.69
Scan method	$\omega - 2\theta$
Data collected	$h: -13, 13; k: 0, 5; l: 0, 13$
Unique reflections	1183
Reflections in refinement	936 ($I \geq 3\sigma(I)$)
Structure solution	Direct methods and Fourier
Refinement	Full-matrix least-squares
Function minimized	$\sum_w (F_o - F_c)^2$; $w = \frac{1}{4}(\sigma(I))^2 + p^2I$; $p = 0.06$
R	0.035
R_w	0.047
G.O.F.	1.35

TABLE II
 ATOMIC AND THERMAL COORDINATES FOR $\text{LaZr}_2\text{Ni}_4\text{As}_4$ ($\beta_{ij} \times 10^5$)

Atom	x	z	β_{11}	β_{22}	β_{33}	β_{13}	$B_{\text{eq.}} (\text{\AA}^2)$
La	0.75338(6)	0.63423(6)	243(5)	250(30)	158(5)	122(8)	0.527(9)
Zr(1)	0.1055(1)	0.8725(1)	170(8)	560(50)	104(8)	40(10)	0.45(1)
Zr(2)	0.4538(1)	0.8563(1)	203(8)	310(50)	104(8)	120(10)	0.43(1)
Ni(1)	0.3199(1)	0.1133(1)	200(10)	500(70)	80(20)	50(30)	0.46(2)
Ni(2) ^a	0.4099(2)	0.5654(2)	300(10)	870(90)	110(10)	-20(20)	0.69(3)
Ni(3)	0.7248(1)	0.2889(1)	230(10)	770(70)	130(10)	-20(20)	0.62(2)
Ni(4)	0.9809(1)	0.3890(1)	220(10)	930(70)	160(10)	70(20)	0.65(2)
As(1)	0.1650(1)	0.8324(1)	272(9)	290(50)	102(8)	100(10)	0.51(2)
As(2)	0.0849(1)	0.1676(1)	190(8)	470(50)	98(8)	80(10)	0.44(2)
As(3)	0.6997(1)	0.0293(1)	206(8)	100(50)	88(8)	60(10)	0.38(2)
As(4)	0.4817(1)	0.3311(1)	221(9)	290(50)	98(8)	70(10)	0.45(2)

Note. The thermal factor is given by $\exp[-(\beta_{11}h^2 + \beta_{22}k^2 + \beta_{33}l^2 + \beta_{12}hl + \beta_{23}kl + \beta_{13}hl)]$. For all the positions $\beta_{12} = \beta_{23} = 0$ and $y = 0.25$. $B_{\text{eq.}} = \frac{1}{3} \sum_i \sum_j \beta_{ij} \mathbf{a}_i \cdot \mathbf{a}_j$.

^a Occupancy factor is 0.806(3).

direct methods, Fourier difference syntheses, and bond distance calculations for the $\text{LaZr}_2\text{Ni}_4\text{As}_4$ structure determination were taken from the SDP package implemented on a PDP 11/60 minicomputer (20). All the atoms were gradually placed in the $2e$ positions of the space group and, at this stage, the R value was 0.110 ($R_w = 0.137$). By

introducing in the refinement the secondary extinction coefficient and isotropic temperature factors, the R value converged to $R = 0.079$ ($R_w = 0.097$) with an abnormally high temperature factor for a nickel atom ($B = 1.5 \text{\AA}^2$).

In the final cycles, the anisotropic temperature factors were refined together with the occupancy factor of the nickel position ($\tau = 0.80(1)$) and gave a conventional residual R of 0.035 ($R_w = 0.047$).

The final Fourier difference map did not show any peak greater than 1 e/\AA^3 . The atomic and thermal parameters are listed in Table II and the interatomic distances in Table III.

Structural Results

Figure 1 illustrates the crystal structure of $\text{LaZr}_2\text{Ni}_4\text{As}_4$ in projection on the (010) plane. The lanthanum atoms are surrounded by six arsenic atoms in a trigonal prismatic coordination with an average La-As bond distance of 3.06\AA . The zirconium atoms occupy two different sites. The Zr(1) atoms are located in slightly distorted arsenic octahedra; these octahedra are linked as

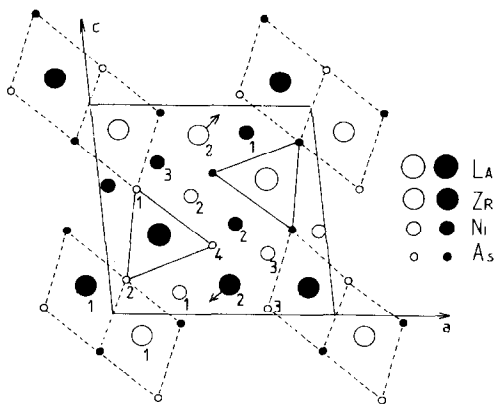


FIG. 1. Crystal structure of $\text{LaZr}_2\text{Ni}_4\text{As}_4$ given in projection on the (010) plane. The full lines emphasize the $[\text{LaAs}_6]$ prisms and the broken lines the $[\text{Zr}(1)\text{As}_6]$ octahedra. Arrows indicate the apex of the $[\text{Zr}(2)\text{As}_6]$ pyramids. Full and open circles are translated from each other by half a period of the projection direction.

TABLE III
MAIN INTERATOMIC DISTANCES (Å) AND THEIR ESTIMATED STANDARD
DEVIATIONS

La	-2As(2)	3.010(1)	Zr(1)-2As(2)	2.704(1)	Zr(2)-Ni(2)	2.705(1)
	-2Ni(2)	3.024(1)	-As(1)	2.751(1)	-As(3)	2.718(1)
	-2As(4)	3.078(1)	-As(2)	2.801(1)	-As(4)	2.769(1)
	-2As(1)	3.090(1)	-2As(3)	2.810(1)	-2As(3)	2.778(1)
	-Ni(3)	3.213(1)	-Ni(1)	2.871(1)	-2Ni(3)	2.857(1)
	-2Ni(1)	3.233(1)	-2Ni(3)	3.098(1)	-Ni(1)	2.890(1)
	-2Ni(4)	3.292(1)	-2Ni(4)	3.172(1)	-2Ni(1)	2.950(1)
	-Ni(2)	3.336(2)			-2Zr(2)	3.364(1)
Ni(1)-2As(3)		2.375(1)	Ni(2)-2As(4)	2.383(1)	Ni(3)-As(3)	2.414(1)
-As(4)		2.413(1)	-As(4)	2.393(2)	-2As(1)	2.438(1)
-As(2)		2.419(1)	-As(1)	2.444(2)	-As(4)	2.464(1)
-Zr(1)		2.871(1)	-Zr(2)	2.705(2)	-Ni(4)	2.556(2)
-Zr(2)		2.890(1)	-2Ni(3)	2.822(1)	-2Ni(2)	2.822(1)
-2Zr(2)		2.950(1)	-2Ni(2)	3.012(2)	-2Zr(2)	2.857(1)
-2La		3.233(1)	-2La	3.024(1)	-2Zr(1)	3.098(1)
			-La	3.336(2)	-La	3.213(1)
Ni(4)-As(2)		2.430(2)	Ni(4)-2Ni(4)	2.856(1)		
-2As(1)		2.451(1)	-2Zr(1)	3.172(1)		
-As(1)		2.453(1)	-2La	3.292(1)		
-Ni(3)		2.556(2)				

pairs via a common edge and generate files along the $[010]$ direction. Such an octahedral arrangement has been previously reported for the Zr₂Ni₃P₃ type (14). The Zr(2) atoms occupy square planar pyramids as found in zirconium containing phosphides as ZrRuP of Fe₂P type (21). The average Zr-As bond distances are identical in pyramidal and octahedral coordination (d Zr-As = 2.76 Å) which is surprising since it is agreed that an octahedral site is larger than a pyramidal one. All of the nickel atoms are tetrahedrally coordinated by arsenic atoms with an average Ni-As bond distance of 2.42 Å. All of these interatomic bond distances compare very well with the sum of the metallic radii for coordination number 12 and the tetrahedral radius of arsenic (d La-As = 3.05 Å, d Zr-As = 2.78 Å, and d Ni-As = 2.42 Å) (22, 23).

No arsenic-arsenic bonds occur in the structure contrary to the numerous metal-metal interactions as reported in Table III.

Comparative Study and Discussion

The structure of LaZr₂Ni₄As₄ is closely related to that of Zr₂Ni₃P₃ because of the occurrence of octahedral together with prismatic, pyramidal, and tetrahedral arsenic polyhedra. Although these two structures have a metal/nonmetal ratio slightly less than two, their nearest neighbor atomic coordination, with the exception of the octahedral environment, obeys the rules which have been defined for a wide family of structures having a metal/nonmetal ratio equal to two (18). These rules are based on the occurrence of metallic triangular units descended from the structures of Fe₂P, Zr₂Fe₁₂P₇, Zr₆Ni₂₀P₁₃, and La₁₂Rh₃₀P₂₁; these units were named units (3:1), (1:6:3), (3:10:6), and (6:15:10), respectively. The combination of similar units linked two by two via a common vertex as linear or zigzag chains has permitted us to describe the structures of Fe₂As, UNi₅Si₃, HoCo₃P₂ (lin-

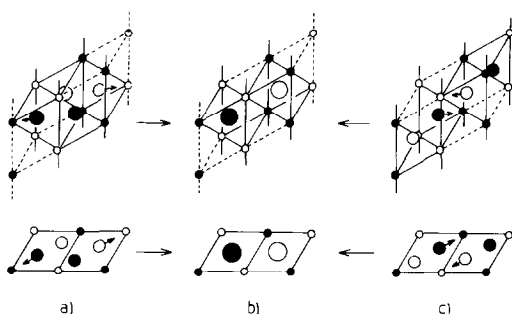
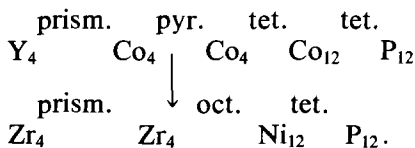


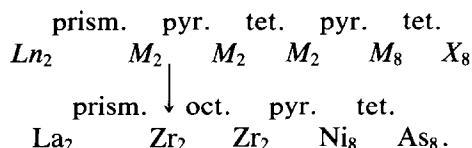
FIG. 2. Various possible occupancies by metal atoms in the "birhombohedral" unit as the sequences: (a) pyr-tet-tet-pyr, (b) oct-oct, and (c) tet-pyr-pyr-tet.

ear chains) and Co_2P , YCo_5P_3 (zigzag chains) (18).

For all of these structures, the arrangement of the chains locally induces isolated metalloid blocks in which metal atoms are distributed as the sequence pyramid-tetrahedron-tetrahedron-pyramid (Fig. 2a). These blocks result from the juxtaposition via a common face of two rhombohedral units; the rhombohedral unit has been defined by R. Fruchart to explain the structures of M_2X and $MM'X$ compounds (24). These "birhombohedral" blocks can also be viewed, along the projection direction, as two octahedral sites having a common edge (Fig. 2b). Thereby, one can imagine that the four atoms in pyramidal and tetrahedral sites within a block can be replaced by two larger and more electropositive ones in octahedral coordination. This mechanism explains the relationship between the structures of YCo_5P_3 and $\text{Zr}_2\text{Ni}_3\text{P}_3$ as shown in Fig. 3. It is illustrated by the developed following formula:



The structure of $\text{LaZr}_2\text{Ni}_4\text{As}_4$, in which zirconium atoms occupy also octahedral sites, can be also deduced by means of such a mechanism. Indeed, this structure derives from a hypothetical " $\text{Ln}_2\text{M}_{14}\text{X}_8$ " one obtained by the alternated combination of (3:1) and (1:6:3) units linked two by two as zigzag chains (Fig. 4). The structural relation can be expressed by:



The two precedent examples show that the substitution of four atoms (two in pyramidal plus two in tetrahedral sites) by two in octahedral sites involves a decrease of the metal/nonmetal ratio as formulated by $Z|(\text{Ln}, \text{M})_{2n}\text{X}_n| \rightarrow Z|(\text{Ln}, \text{M})_{2n-1}\text{X}_n|$ where Z is the number of formula units per cell and n is an integer. This substitution is strongly correlated to a global increase of both electropositivity and size of the metal atoms.

When extending these systematics to the binary structures of Co_2P and Fe_2As where the "birhombohedral" units are not isolated, it appears that the substitution in these structures of cobalt and iron atoms by larger and more electropositive ones leads to binaries with formulae MX . In the case of Co_2P , the substitution will lead to a stacking of NiAs type shown as the orthohexagonal unit cell (Fig. 5a), whereas in the case of Fe_2As , the resulting stacking will be of rocksalt type as the tetragonal body-centered unit cell (Fig. 5b). These systematics may explain numerous features for binary monpnictides MX :

—When M is large and strongly electropositive (rare earth), the corresponding MX compound adopts the rocksalt-like structure which is known to be more ionic and the M_2X binary does not exist.

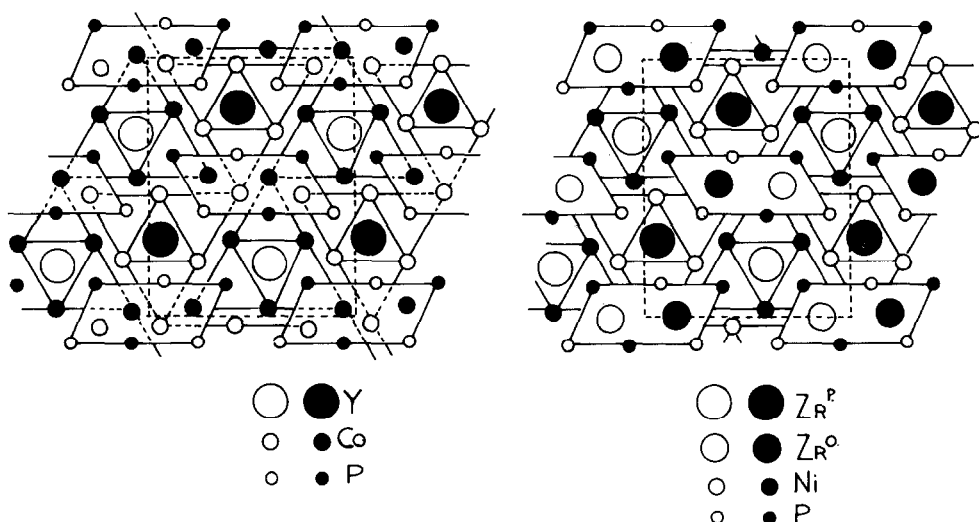


FIG. 3. Structural relationship between the YCo_3P_3 and $\text{Zr}_2\text{Ni}_3\text{P}_3$ types. The "birhombohedral" units are emphasized. Full and open circles are translated from each other by half a period of the projection direction.

—When M is small and not very electropositive (iron, cobalt, nickel, etc.), as in the NiAs type or its derivative of MnP type, more covalence occurs. In addition, metal-rich compounds such as M_2X are known.

—When M presents intermediate size and electropositivity (titanium, zirconium, hafnium, etc.), the corresponding mononitrides MX crystallize in the TiP-type structure which has been described as a

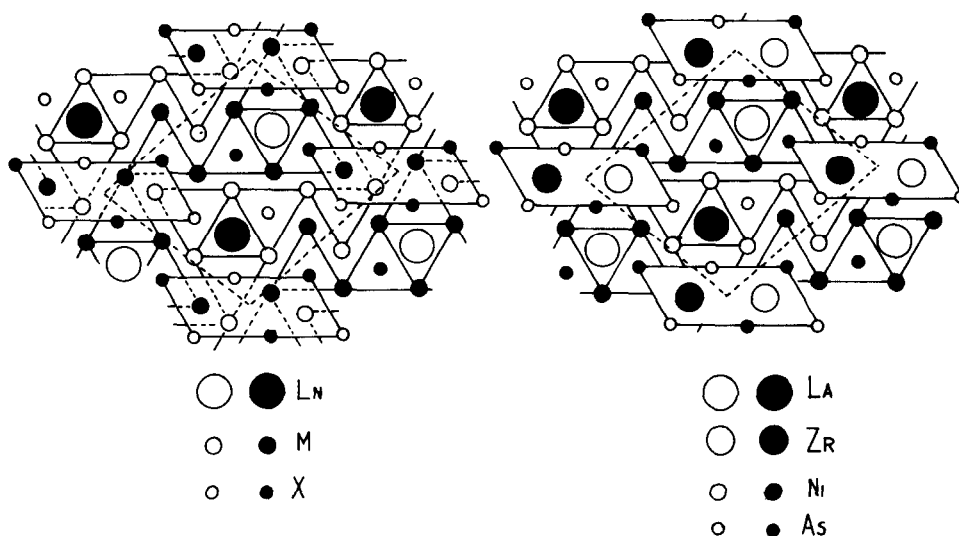


FIG. 4. Structural relationship between the " $\text{Ln}_2\text{M}_{14}\text{X}_8$ " and $\text{LaZr}_2\text{Ni}_4\text{As}_4$ types. Same remarks as for Fig. 3.

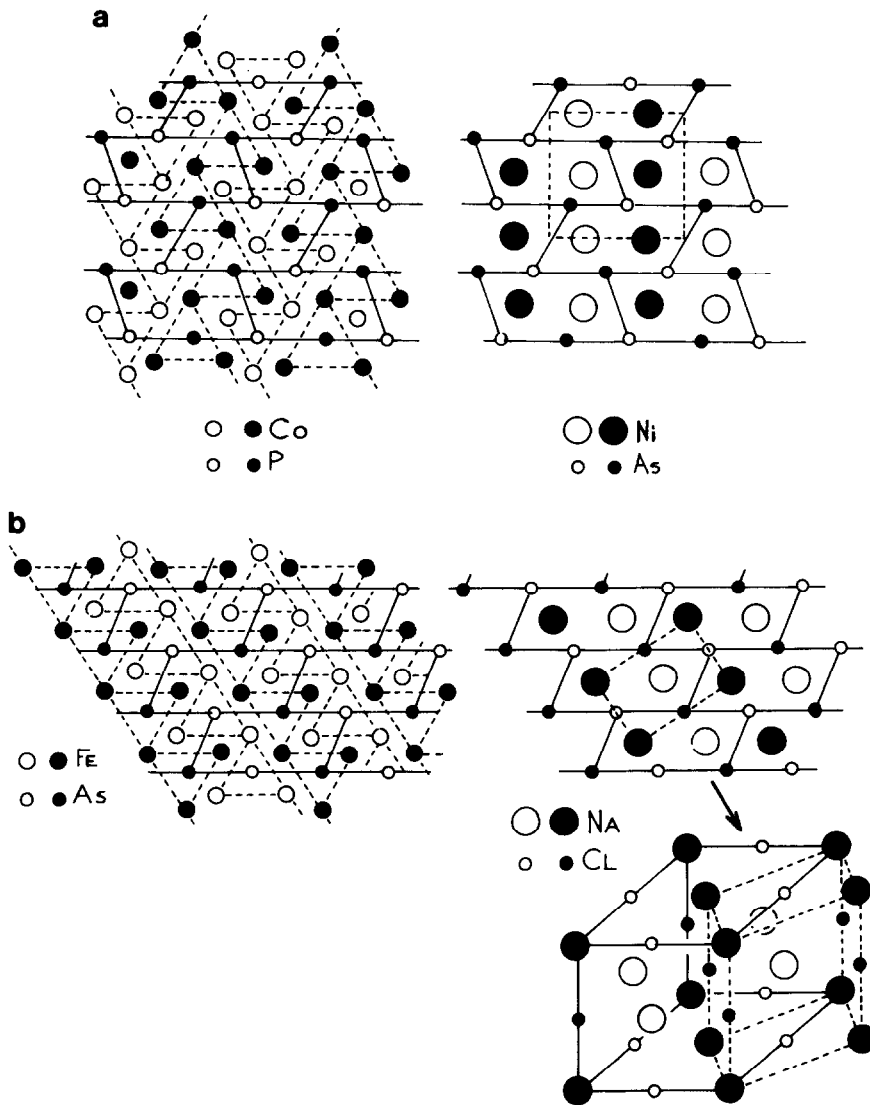


FIG. 5. Structural relationship between the structure types: (a) Co_2P and NiAs , (b) Fe_2As and NaCl (rocksalt type). The tetragonal body-centered subcell of rocksalt type is emphasized.

mixture of NiAs and rocksalt types (25). In that case, no M_2X compounds have been reported in the literature.

All of these considerations have been recently confirmed by the discovery of a new family of ternary compounds Ln_2NiX_2 (15) which exhibit a TiP-like structure. The de-

crease of both size and electropositivity of the LnX network (rocksalt type) by nickel insertion is responsible for this structural stabilization.

In a general way, the structural evolution from the rocksalt to the NiAs types through the TiP one for binaries MX belonging to the IIIa–VIIIa columns of the periodic ta-

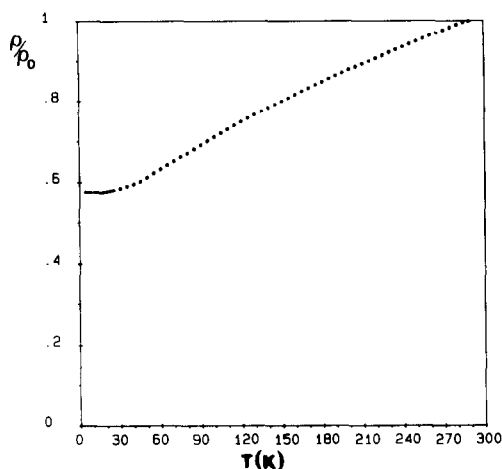


FIG. 6. Normalized resistivity curve as a function of the temperature for $\text{LaZr}_2\text{Ni}_4\text{As}_4$.

ble strongly depends on the size and the electropositivity of the metals.

Physical Properties of $\text{LaZr}_2\text{Ni}_4\text{As}_4$

The susceptibility measurements on $\text{LaZr}_2\text{Ni}_4\text{As}_4$ were made with a SQUID magnetometer, using a polycrystalline sample weighing 80 mg, as a function of temperature from 5 to 300 K at a field strength of 1 K/Oe. This compound exhibits almost a temperature-independent paramagnetism with a susceptibility at room temperature of $0.7 \cdot 10^{-6} \text{ emu g}^{-1}$. This indicates that there is no paramagnetic contribution of the (Zr, Ni, As) sublattice.

Single crystals of $\text{LaZr}_2\text{Ni}_4\text{As}_4$ have been studied by electrical measurement. The experiment was performed by the four-point method using silver painted contacts and an alternating current in the temperature range 4–300 K. The resistivity for $\text{LaZr}_2\text{Ni}_4\text{As}_4$, which is almost linear with temperature down to 30 K, obeys an αT^2 law below this temperature. This indicates a metallic behavior for this compound (Fig. 6).

Conclusion

The examination of the structure of $\text{LaZr}_2\text{Ni}_4\text{As}_4$ brings new perspectives in transition metal lanthanoid pnictides chemistry. Indeed, the classification scheme we recently proposed to describe structures having a metal/nonmetal ratio of 2 can now be extended to related structures with lower metal contents. This can be explained from a steric and electropositive point of view in terms of localized modifications of the metal coordination. As a consequence, in addition to the usual metal coordination such as trigonal prismatic, pyramidal, tetrahedral, and triangular, the following new ones can be mentioned: octahedral, square-planar, cubic, monocapped trigonal prismatic, etc. Collation of these principles will form the subject of a future paper.

Acknowledgments

The authors are indebted to Dr. O. Pena and Dr. J. Padiou for the magnetic and electrical measurements.

References

1. R. MARCHAND AND W. JEITSCHKO, *J. Solid State Chem.* **24**, 351 (1978).
2. W. JEITSCHKO AND M. REEHUIS, *J. Phys. Solids* **48**, 667 (1986).
3. W. JEITSCHKO, W. K. HOFMANN, AND L. J. TERBUCHTE, *J. Less-Common Met.* **137**, 133 (1988).
4. E. H. EL GHADRAOUI, J. Y. PIVAN, R. GUÉRIN, O. PENA, J. PADIYOU, AND M. SERGENT, *Mater. Res. Bull.* **23**, 1345 (1988).
5. D. J. BRAUN AND W. JEITSCHKO, *Acta Crystallogr. Sect. B* **34**, 2069 (1978).
6. W. K. HOFMANN AND W. JEITSCHKO, *J. Solid State Chem.* **51**, 152 (1984).
7. W. JEITSCHKO, D. J. BRAUN, R. H. ASHCRAFT, AND R. MARCHAND, *J. Solid State Chem.* **25**, 309 (1978).
8. W. JEITSCHKO AND B. JABERG, *Z. Anorg. Allg. Chem.* **467**, 95 (1980).
9. J. Y. PIVAN, R. GUÉRIN, J. PADIYOU, AND M. SERGENT, *J. Less-Common Met.* **118**, 191 (1986).
10. R. GUÉRIN, E. H. EL GHADRAOUI, J. Y. PIVAN, J.

- PADIOU, AND M. SERGENT, *Mater. Res. Bull.* **19**, 1257 (1984).
11. R. MADAR, P. CHAUDOUET, E. DHAHRI, J. P. SÉNATEUR, R. FRUCHART, AND B. LAMBERT, *J. Solid State Chem.* **56**, 335 (1985).
 12. J. Y. PIVAN, R. GUÉRIN, AND M. SERGENT, *Inorg. Chem. Acta* **109**, 221 (1985).
 13. J. Y. PIVAN, R. GUÉRIN, AND M. SERGENT, *Mater. Res. Bull.* **20**, 887 (1985).
 14. E. H. EL GHADRAOUI, J. Y. PIVAN, R. GUÉRIN, J. PADIOU, AND M. SERGENT, *J. Less-Common Met.* **105**, 187 (1985).
 15. E. H. EL GHADRAOUI, J. Y. PIVAN, R. GUÉRIN, AND M. SERGENT, *Mater. Res. Bull.* **23**, 891 (1988).
 16. E. H. EL GHADRAOUI, J. Y. PIVAN, AND R. GUÉRIN, *Mater. Res. Bull.*, in press.
 17. R. MADAR, V. GHETTA, E. DHAHRI, P. CHAUDOUET, AND J. P. SÉNATEUR, *J. Solid State Chem.* **66**, 73 (1987).
 18. J. Y. PIVAN, R. GUÉRIN, AND M. SERGENT, *J. Solid State Chem.* **68**, 11 (1987).
 19. E. H. EL GHADRAOUI, J. Y. PIVAN, R. GUÉRIN, AND M. SERGENT, *J. Phys. Chem. Solids*, in press.
 20. B. A. FRENZ, in "Computing in Crystallography" (H. Schenk, R. Olthof-Hazekamp, M. Van Koningsveld, and G. C. Bassi, Eds.), Delft Univ. Press (1978).
 21. H. BARZ, H. C. KU, G. P. MEISNER, Z. FISK, AND B. T. MATTHIAS, *Proc. Natl. Acad. Sci. USA* **77**, 3132 (1980).
 22. F. LAVES, "Theory of Alloys Phases," Amer. Soc. Met., OH (1956).
 23. L. PAULING, "The Nature of the Chemical Bond," 3rd ed., Cornell Univ. Press, Ithaca, NY (1960).
 24. R. FRUCHART, *Ann. Chim. Fr.* **7**, 563 (1982).
 25. F. JELLINEK, *Oster. Chem. Zeit.*, 311 (1960).